SRC TR 86-73

Optimal State Estimation in the Transesterification Stage of a Continuous Polyethylene Terephthalate Condensation Polymerization Process

by

K. Y. Choi and A. A. Khan

Optimal State Estimation in the Transesterification Stage of a Continuous Polyethylene Terephthalate Condensation Polymerization Process

by

K. Y. Choi* and A. A. Khan

Department of Chemical and Nuclear Engineering
and Systems Research Center
University of Maryland
College Park, MD 20742

---

*To whom correspondence should be addressed

Abstract

This paper describes an application of the extended Kalman filter algorithm to the state estimation of the melt transesterification stage of a continuous polyethylene terephthalate condensation polymerization process. When only two on-line measurements of reaction variables are used for state estimation, the prediction of reaction rates and product concentrations are unsatisfactory. When such limited on-line measurements are supplemented by five additional off-line measurements of various functional group concentrations, the overall performance of the state estimator is greatly improved. It has been shown that the analysis delay of 24 hours is quite adequate for accurate state estimation of the process. In particular, the concentration of unwanted side product such as diethylene glycol(DEG) was predicted precisely. The simulation results indicate that the extended Kalman filter can be used successfully with a dynamic transesterification process model for precise control of reaction product quality.

INTRODUCTION

Polyethylene terephthalate (PET) is one of the fastest growing thermoplastic polyesters used extensively for fibers, films, bottles, injection molded parts and other products. PET is manufactured by a step growth melt polymerization process which comprises three reaction steps: (i) melt transesterification of dimethyl terephthalate (DMT) with ethylene glycol (EG), (ii) prepolymerization at 250-300^{o}C and ~30 mmHg, (iii) finishing polymerization at 280 - 300^{o}C and ~1 mmHg. Biaxially oriented PET films contain a high degree of molecular orientation which improves its tensile strength, clarity, stiffness, chemical resistance and barrier properties. Such PET films have found commercial application not only in the traditional areas of magnetic tape media and photographic film coating, but also in such diversified areas as food packaging and electrical applicance insulation. PET resins may also be crystallizable (CPET) or reinforced with glass fibers and minerals for many additional engineering applications.

Due to the stringent industrial product specifications that today's polymers and engineering plastics must meet, the need for fine tuning the polymer properties through more effective reactor operation is now more acute than ever. For instance, in order to produce PET resins offering a combination of high strength, stiffness, dimensional stability, chemical and heat resistance, and good electrical properties, the polymer molecular weight and undesirable side product concentrations must be controlled within limits that would not damage industrial end requirements. The presence of diethylene glycol (DEG), even in small concentrations

(1~2 wt %), in final polymer products causes decreased polymer crystallinity, resulting in lowered melting points, reduced heat resistance, and decreased thermal oxidative and UV light stability. Such polymer property variables, in most instances, are very difficult or impossible to measure on-line. Thus, it is very difficult to control polymer product quality when all that is available are only infrequent and delayed off-line laboratory measurements. For this reason, much current research interest in the area of polymerization process control is devoted to a study of estimation theory and subsequent real time application.

Optimal state estimation, the process of extracting information concerning a parameter or function from noise-corrupted observations, has recently found extensive application in many areas such as chemical processes, telecommunication and satellite orbit determination [Wells (1971), Schuler (1985), Nahi (1976), Sage and Melsa (1971)]. In order to apply the techniques of estimation theory to a particular engineering problem, an appropriate mathematical model must be constructed for the system of concern. Most chemical processes, due to their highly nonlinear nature, cannot be readily modeled and thus defining control strategies becomes cumbersome. Since the implementation of estimation algorithms is based primarily on system state observations or some function thereof, the use of the extended Kalman filter can aid in parameter estimation and model development given that a measure of the inaccuracy of the model is directly obtainable.

The objective of this paper is to model the first stage of a PET condensation polymerization process and to develop an optimal state estimator. DMT conversion and product composition distribution will be estimated using the extended Kalman filter. The performance of the state estimator will be illustrated through numerical simulation of the dynamic model.

MODEL DEVELOPMENT

Consider the process flow diagram for a continuous transesterification process shown in Figure 1. Molten DMT is fed to the ester interchange reactor which is kept under an inert atmosphere within the temperature range 180-200^{o}C. Ethylene glycol is passed in a similar fashion to the reactor from an EG storage tank. The metal acetate catalyst (e.g. zinc acetate) is injected into the EG feed stream from a catalyst storage vessel. The resultant vapors (mostly methanol, EG and trace amounts of other volatile side products) from the combination of DMT and EG to produce BHET are rectified in the distillation column; thus, EG is refluxed back into the reactor. The more volatile components in the vapor phase are condensed in a condenser and their amounts are used to gauge the extent of reaction in the liquid phase. The transesterification product is transferred to the prepolycondesnation reactor which is maintained between 10$\sim$30 mmHg and 280-300^{o}C. The polymer melt is pumped to the finishing polymerization reactor, usually an extruder type or a wiped film reactor.

Of the large number of possible chemical reactions postulated for the transesterification stage, we shall consider four of the most important ones. For an exhaustive evaluation of the transesterification reaction chemistry, the works of Ravindranath and Mashelkar (1981, 1982(a), (b)) should prove to be very instructive. The motivation concerning the choice and number of reactions is to reduce the complexity posed by considering every possible reactions but also to maintain a

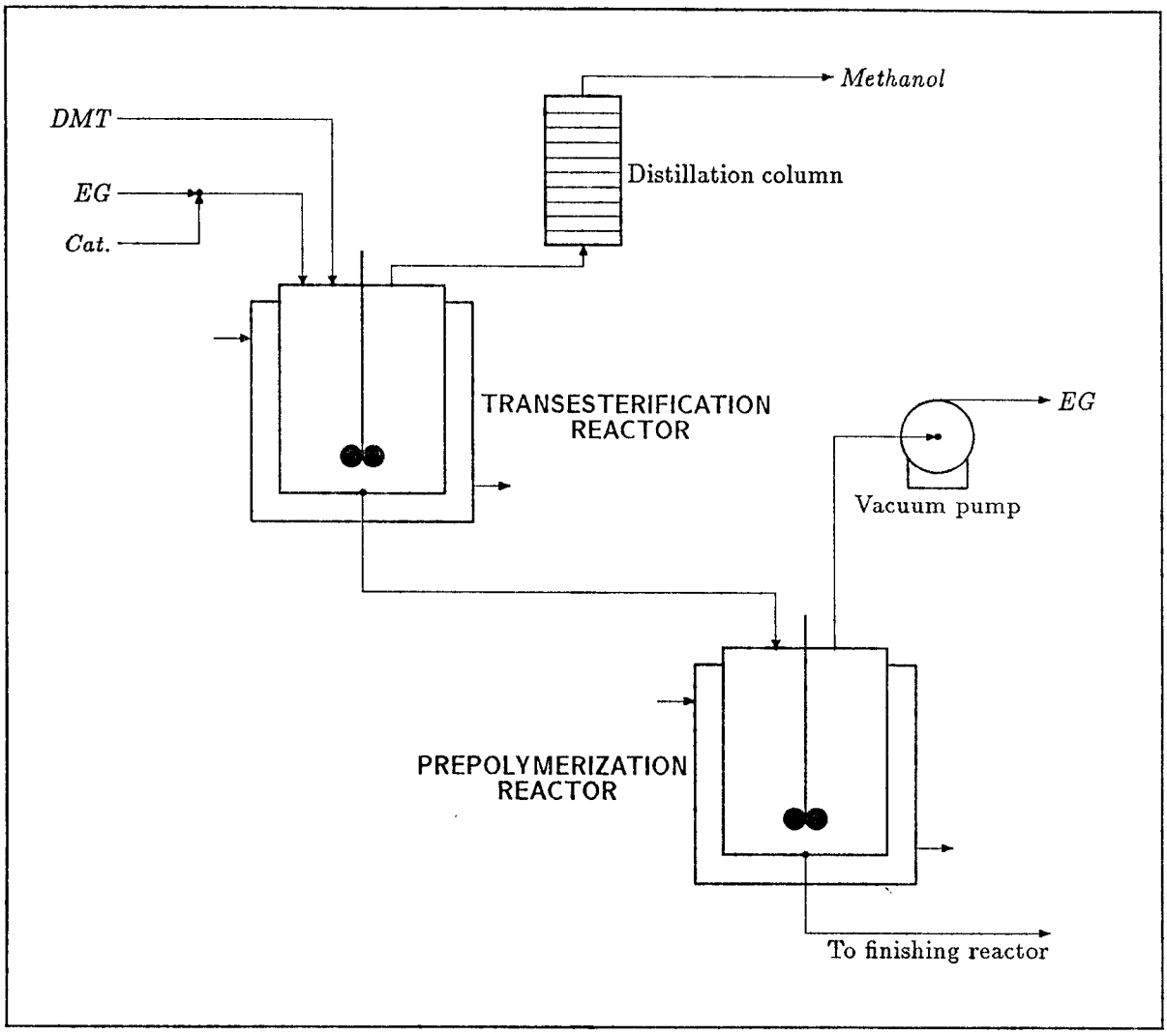

Figure 1. Schematic diagram of continuous melt PET polymerization process.

realistic workable model which can be used for process control purposes. Assuming that no oligomerization occurs in this stage, the main transesterification reactions are

$$D + G \underset{k'_1}{\overset{k_1}{\rightleftharpoons}} R_1 + M \qquad (1)$$

$$R_1 + G \underset{k'_2}{\overset{k_2}{\rightleftharpoons}} P_1 + M \qquad (2)$$

The chemical formulae for the symbols are shown in Table 1. When the continuous removal of liberated methanol (M) is efficiently performed, the two reactions above may be conveniently approximated as irreversible reactions. In addition to main reactions (1) and (2), important side reactions lead to the formation of diethylene glycol (DEG), which often deteriorates the properties of the final PET produced (e.g. the melting point of PET decreases by $5^{o}C$ for each weight percent of DEG incorporated, and the presence of small amounts of DEG causes undersirable coloring problems [Ravindranath and Mashelkar, 1981]). Therefore, the side reactions considered in this work deal directly with the formation of DEG,

$$R_1 + G \xrightarrow{k_3} T_1 + G_D \qquad (3)$$

$$P_1 + G \xrightarrow{k_3} Q_1 + G_d \qquad (4)$$

Note that the reactivities of reactions (3) and (4) have been assumed to be the same according to Ravindranath and Mashelkar (1981). The temperature dependence of the rate constants is accounted for in the standard Arrhenius rate expression (i.e. $k_i = A_i\, e^{-E_i/RT}$).

Table 1: *Chemical formulae for the transesterification model.*

Dimethyl terephthalate (DMT or D)

Ethylene glycol (EG or G)

$$HOCH_2CH_2OH$$

Diethylene glycol (DEG or G_D)

$$HOCH_2CH_2OCH_2CH_2OH$$

Methanol (M)

$$CH_3OH$$

Bis-hydroxyethyl terephthalate (BHET or P_1)

Hydroxyethyl terephthalic acid (HTPA or Q_1)

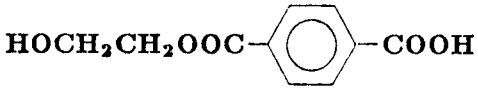

Methyl-hydroxyethyl terephthalate (MHET or R_1)

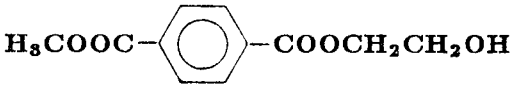

Methyl terephthalic acid (MTPA or T_1)

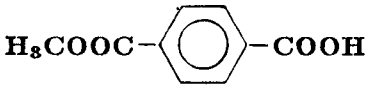

Modeling Equations

Unlike most of the other works on the modeling of the transesterification stage, the catalyst concentration in the reactor has not been incorporated into the frequency factor of the rate constant and its effect on the reactor states will be considered independently. The material balances for each species and the energy balance take the following form:

Material balances:

$$V\frac{dD}{dt'} = D_o q_o - Dq_1 - k_1 V C_{cat} DG \tag{5}$$

$$V\frac{dG}{dt'} = G_o q_o - Gq_1 - k_1 V C_{cat} G - (k_2 + k_3) V C_{cat} R_1 G - k_3 V C_{cat} P_1 G \tag{6}$$

$$V\frac{dG_D}{dt'} = G_{D_o} q_o - G_D q_1 + k_3 V C_{cat} G(R_1 + P_1) \tag{7}$$

$$V\frac{dR_1}{dt'} = R_{1_o} q_o + k_1 V C_{cat} DG - (k_2 + k_3) V C_{cat} R_1 G \tag{8}$$

$$V\frac{dP_1}{dt'} = P_{1_o} q_o - P_1 q_1 + k_2 V C_{cat} R_1 G - k_3 V C_{cat} P_1 G \tag{9}$$

$$V\frac{dQ_1}{dt'} = Q_{1_o} q_o - Q_1 q_1 + k_3 V C_{cat} P_1 G \tag{10}$$

$$V\frac{dT_1}{dt'} = T_{1_o} q_o - T_1 q_1 + k_3 V C_{cat} R_1 G \tag{11}$$

$$V\frac{dC_{cat}}{dt'} = C_{cat_o} q_o - C_{cat} q_1 \tag{12}$$

Energy balance:

$$\begin{aligned}\rho C_p V\frac{dT}{dt'} = {} & \rho_o C_p q_o (T_o - T_r) - \rho_1 C_p q_1 (T - T_r) - U_o A_c (T - T_h) \\ & - V\left[k_1 C_{cat} DG\Delta H_1 + k_2 C_{cat} R_1 G\Delta H_2 + k_3 C_{cat} R_1 G\Delta H_3 + k_3 C_{cat} P_1 G\Delta H_4\right] \\ & - V\left[\Delta H_v(T_r) + C_{p_{Mg}}(T - T_r)\right]\left[k_1 C_{cat} DG + k_2 C_{cat} R_1 G\right]\end{aligned} \tag{13}$$

Since the reactor is operated at constant reactor volume, the following equation is valid for the effluent stream flow rate which is subject to vary according to the methanol vapor removal rate:

$$q_1 = q_o - \hat{V}_M(k_1 VC_{cat} DG + k_2 VC_{cat} R_1 G) \qquad (14)$$

where $\hat{V}_M$ denotes the molar volume of methanol.

It is convenient to put the transesterification modeling equations (5)-(14) into dimensionless form. For this purpose, the dimensionless variables and parameters defined in Table 2 were substituted into the material and energy balances, resulting in the following dimensionless dynamic modeling equations:

$$\frac{dx_1}{dt} = -1 + q(1-x_1) + z_2 Dar_1(1-x_1)(1-x_2)(1-x_8)\exp\left[\frac{\Gamma_1 x_9}{1+x_9/\Gamma}\right] \qquad (15)$$

$$\begin{aligned}\frac{dx_2}{dt} = {} & -1 + q(1-x_2) + Dar_1(1-x_1)(1-x_2)(1-x_8)\exp\left[\frac{\Gamma_1 x_9}{1+x_9/\Gamma}\right] \\ & + Dar_2(1-x_2)x_4(1-x_8)\exp\left[\frac{\Gamma_2 x_9}{1+x_9/\Gamma}\right] + Da(1-x_2)x_4(1-x_8)\exp\left[\frac{x_9}{1+x_9/\Gamma}\right] \\ & + Da(1-x_2)x_5(1-x_8)\exp\left[\frac{x_9}{1+x_9/\Gamma}\right]\end{aligned} \qquad (16)$$

$$\frac{dx_3}{dt} = z_3 - qx_3 + z_2 Da(1-x_2)(x_4+x_5)(1-x_8)\exp\left[\frac{x_9}{1+x_9/\Gamma}\right] \qquad (17)$$

$$\begin{aligned}\frac{dx_4}{dt} = {} & z_4 - qx_4 + z_2 Dar_1(1-x_1)(1-x_2)(1-x_8)\exp\left[\frac{\Gamma_1 x_9}{1+x_9/\Gamma}\right] \\ & - z_2 Dar_2(1-x_2)x_4(1-x_8)\exp\left[\frac{\Gamma_2 x_9}{1+x_9/\Gamma}\right] - z_2 Da(1-x_2)x_4(1-x_8)\exp\left[\frac{x_9}{1+x_9/\Gamma}\right]\end{aligned} \qquad (18)$$

$$\frac{dx_5}{dt} = z_5 - qx_5 + z_2 Dar_2(1-x_2)x_4(1-x_8)\exp\left[\frac{\Gamma_2 x_9}{1+x_9/\Gamma}\right] \tag{19}$$
$$- z_2 Da(1-x_2)x_5(1-x_8)\exp\left[\frac{x_9}{1+x_9/\Gamma}\right]$$

$$\frac{dx_6}{dt} = z_6 - qx_6 + z_2 Da(1-x_2)x_5(1-x_8)\exp\left[\frac{x_9}{1+x_9/\Gamma}\right] \tag{20}$$

$$\frac{dx_7}{dt} = z_7 - qx_7 + z_2 Da(1-x_2)x_4(1-x_8)\exp\left[\frac{x_9}{1+x_9/\Gamma}\right] \tag{21}$$

$$\frac{dx_8}{dt} = -1 + q(1-x_8) \tag{22}$$

$$\frac{dx_9}{dt} = y_4(y_1+y_7) - y_5 q(x_9+y_7) - B_1 Dar_1(1-x_1)(1-x_2)(1-x_8)\exp\left[\frac{\Gamma_1 x_9}{1+x_9/\Gamma}\right] \tag{23}$$
$$- B_2 Dar_2(1-x_2)x_4(1-x_8)\exp\left[\frac{\Gamma_2 x_9}{1+x_9/\Gamma}\right] - B_3 Da(1-x_2)x_4(1-x_8)\exp\left[\frac{x_9}{1+x_9/\Gamma}\right]$$
$$- B_4 Da(1-x_2)x_5(1-x_8)\exp\left[\frac{x_9}{1+x_9/\Gamma}\right] - \beta(x_9-y_2)$$
$$- \left(B_v + y_6(x_9+y_7)\right)\left(Dar_1(1-x_1)(1-x_2)(1-x_8)\exp\left[\frac{\Gamma_1 x_9}{1+x_9/\Gamma}\right]\right.$$
$$\left. + Dar_2(1-x_2)x_4(1-x_8)\exp\left[\frac{\Gamma_2 x_9}{1+x_9/\Gamma}\right]\right)$$

where

$$q = 1 - y_3 Dar_1(1-x_1)(1-x_2)(1-x_8)\exp\left[\frac{\Gamma_1 x_9}{1+x_9/\Gamma}\right]$$
$$- y_3 Dar_2(1-x_2)x_4(1-x_8)\exp\left[\frac{\Gamma_2 x_9}{1+x_9/\Gamma}\right] \tag{24}$$

Table 2: *Dimensionless parameters.*

$$x_1 = \frac{D_o - D}{D_o} \qquad x_2 = \frac{G_o - G}{G_o} \qquad x_3 = \frac{G_D}{D_o}$$
$$x_4 = \frac{R_1}{D_o} \qquad x_5 = \frac{P_1}{D_o} \qquad x_6 = \frac{Q_1}{D_o}$$
$$x_7 = \frac{T_1}{D_o} \qquad x_8 = \frac{C_{cat_o} - C_{cat}}{C_{cat_o}} \qquad x_9 = \frac{(T - T_k)\Gamma}{T_k}$$

$$y_1 = \frac{(T_o - T_k)\Gamma}{T_k} \qquad y_2 = \frac{(T_h - T_k)\Gamma}{T_k} \qquad y_3 = G_o \hat{V}_M$$
$$y_4 = \rho_o/\rho \qquad y_5 = \rho_1/\rho \qquad y_6 = \frac{C_{p_{Mg}} G_o}{\rho C_p}$$
$$y_7 = \frac{(T_k - T_r)\Gamma}{T_k}$$

$$z_2 = G_o/D_o \qquad z_3 = G_{D_o}/D_o \qquad z_4 = R_{1_o}/D_o$$
$$z_5 = P_{1_o}/D_o \qquad z_6 = Q_{1_o}/D_o \qquad z_7 = T_{1_o}/D_o$$

$$B_1 = \frac{\Delta H_1 G_o \Gamma}{\rho C_p T_k} \qquad B_2 = \frac{\Delta H_2 G_o \Gamma}{\rho C_p T_k} \qquad B_3 = \frac{\Delta H_3 G_o \Gamma}{\rho C_p T_k}$$
$$B_4 = \frac{\Delta H_4 G_o \Gamma}{\rho C_p T_k} \qquad B_v = \frac{\Delta H_v(T_r) G_o \Gamma}{\rho C_p T_k} \qquad Da = k_3(T_k)\theta D_o C_{cat_o}$$

$$r_1 = \frac{k_1(T_k)}{k_3(T_k)} \qquad r_2 = \frac{k_2(T_k)}{k_3(T_k)} \qquad t = \frac{t'}{\theta}$$

Greek letters:

$$\Gamma = \frac{E_3}{RT_k} \qquad \Gamma_1 = \frac{E_1}{E_3} \qquad \Gamma_2 = \frac{E_2}{E_3}$$
$$\theta = \frac{V}{q_o} \qquad \beta = \frac{U_o A_c}{\rho C_p q_o}$$

Implicit assumptions in the model include perfect backmixing and constant physical properties within the temperature range of interest.

All the measurements whether on-line or off-line are assumed to contain random noise (i.e. zero mean and uncorrelated in time). If on-line measurements are made, then the measured quantities will be the amount of methanol produced per unit time and the reactor temperature. In dimensionless form these take the following form (y_{mi} signifies a measured variable),

Methanol flow rate:
$$y_{m_1} = y_3 Dar_1(1-x_1)(1-x_2)(1-x_8)\exp\left[\frac{\Gamma_1 x_9}{1+x_9/\Gamma}\right] + y_3 Dar_2(1-x_2)x_4(1-x_8)\exp\left[\frac{\Gamma_2 x_9}{1+x_9/\Gamma}\right] \quad (25)$$

Reaction temperature:
$$y_{m_2} = x_9 + 1 \quad (26)$$

If, in addition, the on-line measurements are supplemented with off-line analysis (i.e., delayed laboratory analysis), then more information about the actual reactor states may be ascertained. The experimental procedures required for determining the concentrations of the various species involved in the transesterification reactions are well described by Yamada et. al. (1986). A mathematical adaption of these off-line measurements in dimensionless form is

$$y_{m3} = 1 - x_2 \quad (27)$$

$$y_{m4} = x_3 \quad (28)$$

$$y_{m5} = x_6 + x_7 \quad (29)$$

$$y_{m6} = x_4 + 2x_5 + x_6 \quad (30)$$

$$y_{m7} = 2(1-x_1) + 2x_4 + 2x_5 + x_6 + x_7 \quad (31)$$

where y_{m3} = free EG concentration in the reaction mixture, y_{m4} = DEG concentration, y_{m5} = carboxyl end group concentration, y_{m6} = hydroxyl end group concentration, and y_{m7} = saponification value.

The system of modeling equations described above may then be condensed down to the following form in compact vector notation

$$\underline{\dot{x}} = \underline{f}\ (\underline{x},t) \qquad (32)$$

$$\underline{y}_m = \underline{h}\ (\underline{x},t) \qquad (33)$$

where $\underline{f}$ is the system state model and $\underline{h}$ is the system measurement model given by eqs. (25) and (26) on a semi-continuous basis and by eqs. (27)-(31) on a discrete basis.

The Extended Kalman Filter

Although the use of state estimation techniques to reconstruct the unknown system states has become standard practice, especially in the fields of electrical and aeronautical engineering, Kalman and Bucy laid the theoretical groundwork for finite-time optimal filtering for linear systems with random white noise not more than thirty years ago [Kalman (1960), Kalman and Bucy (1961)]. Their research was subsequently extended to nonlinear systems and is now contained in pertinent references [Jazwinski (1970), Nahi (1976), Sage and Melsa (1971), Ray (1981)]. Since most chemical processes are nonlinear in nature, this section concerns the development of the discrete extended Kalman filter.

In general, the filter equations specify an optimal estimate of the states of a dynamic system observed sequentially in the presence of white noise (zero-mean and uncorrelated in time).

The estimate obtained at each time is the least square estimate of each state. Suppose that the system and observation models are given by

$$\dot{\underline{x}}(t) = \underline{f}[\underline{x}(t), t] + \underline{w}(t) \tag{34}$$

$$\underline{y}_m(t) = \underline{h}[\underline{x}(t), t] + \underline{v}(t) \tag{35}$$

$$\underline{x}(0) = \underline{x}_o + \underline{w}_o \tag{36}$$

where $\underline{x}(t)$ is the n-dimensional state vector, $\underline{f}(\underline{x},t)$ is the n-dimensional vector-valued function, $\underline{y}_m(t)$ is the m-dimensional observation vector, $\underline{w}(t)$ is the n-dimensional plant-noise vector, and $\underline{v}(t)$ is the m-dimensional observation-noise vector. The vectors $\underline{v}$ and $\underline{w}$ are zero-mean white Gaussian noise processes assumed to be independent of each other. The discrete formulation is given by

$$\underline{x}(t_{k+1}) = \underline{F}[\underline{x}(t_k), t_k] + \underline{w}(t_k) \tag{37}$$

$$\underline{y}_m(t_k) = \underline{h}[\underline{x}(t_k), t_k] + \underline{v}(t_k) \tag{38}$$

The discrete and continuous formulations are related by the following nonrigorous limits [Sage and Melsa (1971)]

$$\underline{f}[\underline{x}(t), t] = \lim_{\substack{\Delta t \to 0 \\ t_k \to t}} \frac{1}{\Delta t} \{\underline{F}[\underline{x}(t_k), t_k] - \underline{x}(t_k)\} \tag{39}$$

$$\underline{h}[\underline{x}(t), t] = \lim_{\substack{\Delta t \to 0 \\ t_k \to t}} \{\underline{h}[\underline{x}(t_k), t_k]\} \tag{40}$$

This means that

$$\underline{F}[\underline{x}(t_k), t_k] = \underline{x}(t_k) + \int_{t_k}^{t_{k+1}} \underline{f}[\underline{x}(t), t]\, dt \tag{41}$$

If the Euler method of integration is used to evaluate this integral (i.e., $\underline{f}$ is constant over the interval), then eq. (41) is reduced to the simple form

$$\underline{\mathbf{F}}[\underline{\mathbf{x}}(t_k), t_k] = \underline{\mathbf{x}}(t_k) + \underline{\mathbf{f}}[\underline{\mathbf{x}}(t), t]\Delta t \tag{42}$$

where Δt is the sampling interval. The extended Kalman filter determines the state estimate that minimizes the following least square objective function,

$$I = \frac{1}{2}\underline{\mathbf{X}}^T \underline{\underline{\mathbf{P}}}_o^{-1} \underline{\mathbf{X}} + \frac{1}{2}\Delta t \sum_{j=0}^{k} (\underline{\underline{\mathbf{\Psi}}}^T \underline{\underline{\mathbf{R}}}^{-1} \underline{\underline{\mathbf{\Psi}}} + \underline{\mathbf{Y}}^T \underline{\underline{\mathbf{Q}}}^{-1} \underline{\mathbf{Y}}) \tag{43}$$

where

$$\begin{aligned} \underline{\mathbf{X}} &= [\underline{\mathbf{x}}(0) - \underline{\mathbf{x}}_o] \\ \underline{\mathbf{Y}} &= [\underline{\mathbf{y}}_m(t_j) - \underline{\mathbf{h}}(\underline{\mathbf{x}}(t_j), t_j)] \\ \underline{\mathbf{\Psi}} &= [\underline{\mathbf{x}}(t_{j+1}) - \underline{\mathbf{F}}(\underline{\mathbf{x}}(t_j), t_j)] \end{aligned} \tag{44}$$

The weighting matricies $\underline{\underline{\mathbf{P}}}_o^{-1}$, $\underline{\underline{\mathbf{R}}}^{-1}$ and $\underline{\underline{\mathbf{Q}}}^{-1}$ are chosen to reflect the errors in the initial estimate, the plant model, and the measuring device. Thus the expected value relations are

$$\begin{aligned} \mathcal{E}[\underline{\mathbf{w}}(t_k)] &= \underline{\mathbf{0}} \\ \mathcal{E}[\underline{\mathbf{v}}(t_k)] &= \underline{\mathbf{0}} \\ \mathcal{E}[\underline{\mathbf{x}}(0)] &= \underline{\mathbf{x}}_o \\ \mathcal{E}[\underline{\mathbf{w}}(t_k)\underline{\mathbf{x}}^T(0)] &= \underline{\underline{\mathbf{0}}} \\ \mathcal{E}[\underline{\mathbf{v}}(t_k)\underline{\mathbf{x}}^T(0)] &= \underline{\underline{\mathbf{0}}} \\ \mathcal{E}[\underline{\mathbf{w}}(t_k)\underline{\mathbf{v}}^T(t_k)] &= \underline{\underline{\mathbf{0}}} \\ \mathcal{E}\left[(\underline{\mathbf{x}}_o - \underline{\mathbf{x}}(0))(\underline{\mathbf{x}}_o - \underline{\mathbf{x}}(0))^T\right] &= \underline{\underline{\mathbf{P}}}_o \\ \mathcal{E}[\underline{\mathbf{w}}(t_k)\underline{\mathbf{w}}^T(t_j)] &= \underline{\underline{\mathbf{R}}}(t_k)\delta_{jk} \\ \mathcal{E}[\underline{\mathbf{v}}(t_k)\underline{\mathbf{v}}^T(t_j)] &= \underline{\underline{\mathbf{Q}}}(t_k)\delta_{jk} \end{aligned} \tag{45}$$

where δ_{jk} is the Kronecker delta function, $\underline{\underline{P}}_o$ is the covariance matrix of the initial state errors, $\underline{\underline{R}}$ is the covariance matrix of the plant noise, and $\underline{\underline{Q}}$ is the covariance matrix of the measurement noise. The extended Kalman filter is then represented, according to Jazwinski (1970), by the recursive relations as follows:

Filter:

$$\underline{\hat{x}}(t_{k+1}|t_{k+1}) = \underline{\hat{x}}(t_{k+1}|t_k) + \underline{\underline{K}}[t_{k+1}, \underline{\hat{x}}(t_{k+1}|t_k)]\left[\underline{y}_m(t_{k+1}) - \underline{h}[t_{k+1}, \underline{\hat{x}}(t_{k+1}|t_k)]\right] \tag{46}$$

One-stage prediction:

$$\underline{\hat{x}}(t_{k+1}|t_k) = \underline{\hat{x}}(t_k|t_k) + \int_{t_k}^{t_{k+1}} \underline{f}[\underline{\hat{x}}(t\,|t_k), t]dt \tag{47}$$

Kalman filter gain:

$$\begin{aligned}\underline{\underline{K}}[t_{k+1}, \underline{\hat{x}}(t_{k+1}|t_k)] = \underline{\underline{P}}(t_{k+1}|t_k)\underline{\underline{M}}^T[t_{k+1}, \underline{\hat{x}}(t_{k+1}|t_k)]\Big[\underline{\underline{M}}[t_{k+1}, \underline{\hat{x}}(t_{k+1}|t_k)]\underline{\underline{P}}(t_{k+1}|t_k) \\ \times \underline{\underline{M}}^T[t_{k+1}, \underline{\hat{x}}(t_{k+1}|t_k)] + \underline{\underline{Q}}(t_{k+1})\Big]^{-1}\end{aligned} \tag{48}$$

Prior error-variance:

$$\underline{\underline{P}}(t_{k+1}|t_k) = \underline{\underline{\Phi}}[t_{k+1}, t_k; \underline{\hat{x}}(t_k|t_k)]\underline{\underline{P}}(t_k|t_k)\underline{\underline{\Phi}}^T[t_{k+1}, t_k; \underline{\hat{x}}(t_k|t_k)] + \underline{\underline{R}}(t_{k+1}) \tag{49}$$

Error-variance:

$$\begin{aligned}\underline{\underline{P}}(t_{k+1}|t_{k+1}) = \Big[\underline{\underline{I}} - \underline{\underline{K}}[t_{k+1}, \hat{\underline{x}}(t_{k+1}|t_k)]\underline{\underline{M}}[t_{k+1}, \hat{\underline{x}}(t_{k+1}|t_k)]\Big]\underline{\underline{P}}(t_{k+1}|t_k) \\ \times \Big[\underline{\underline{I}} - \underline{\underline{K}}[t_{k+1}, \hat{\underline{x}}(t_{k+1}|t_k)]\underline{\underline{M}}[t_{k+1}, \hat{\underline{x}}(t_{k+1}|t_k)]\Big]^T \\ + \underline{\underline{K}}[t_{k+1}, \hat{\underline{x}}(t_{k+1}|t_k)]\underline{\underline{Q}}(t_{k+1})\underline{\underline{K}}^T[t_{k+1}, \underline{\hat{x}}(t_{k+1}|t_k)]\end{aligned} \tag{50}$$

Initial conditions:

$$\underline{\hat{x}}(t_o|t_o) = \underline{\hat{x}}_o \qquad \underline{\underline{P}}(t_o|t_o) = \underline{\underline{P}}_o \tag{51}$$

where $\underline{\underline{\Phi}} = \underline{\underline{J}}_f(t_{k+1} - t_k) + \underline{\underline{I}}$

$\underline{\underline{M}} = \underline{\underline{J}}_h$

The "a priori" estimate, $\underline{x}(t_k|t_k)$, and initial state error covariance, $\underline{\underline{P}}_o$, are used as initial conditions for these recursive equations. Note that the integral in eq. (47) may be evaluated by a number of methods. In this paper, Euler's method is used. $\underline{\underline{J}}_f$ and $\underline{\underline{J}}_h$ denote Jacobian matrices for the state and measurement model equations, respectively. Figure 2 illustrates the foregoing discussion in the fashion of a block diagram.

Wells (1971) and Sage and Melsa (1971) have discussed the impact of filter tuning parameters on the dynamic response of the filter. The initial state estimate and the initial covariance, $\underline{x}(t_o|t_o)$ and $\underline{\underline{P}}_o$, respectively determine the speed of response of the filter. Depending on how much $\underline{x}(t_o|t_o)$ deviates from $\underline{x}_o$ and how large $\underline{\underline{P}}_o$ is, the time required to reach steady state will increase. The $\underline{\underline{R}}$ matrix, containing plant noise covariances, should be large for systems which have dynamics that are not well understood; this has the effect of increasing the steady state error. The observation noise covariance, $\underline{\underline{Q}}$, is set by the measuring devices; however, in cases where $\underline{\underline{Q}}$ is time dependent, it has the opposite effect of $\underline{\underline{R}}$. The Jacobian matrices $\underline{\underline{J}}_f$ and $\underline{\underline{J}}_h$ are obtained from the first terms of linearized functions $\underline{f}$ and $\underline{h}$ using a Taylor series expansion about the current state estimate. Thus, the Jacobian $\underline{\underline{J}}_f$ is given by

$$\underline{\underline{J}}_f = \begin{pmatrix} f_{11} & f_{12} & 0 & f_{14} & 0 & 0 & 0 & f_{18} & f_{19} \\ f_{21} & f_{22} & 0 & f_{24} & f_{25} & 0 & 0 & f_{28} & f_{29} \\ f_{31} & f_{32} & f_{33} & f_{34} & f_{35} & 0 & 0 & f_{38} & f_{39} \\ f_{41} & f_{42} & 0 & f_{44} & 0 & 0 & 0 & f_{48} & f_{49} \\ f_{51} & f_{52} & 0 & f_{54} & f_{55} & 0 & 0 & f_{58} & f_{59} \\ f_{61} & f_{62} & 0 & f_{64} & f_{65} & f_{66} & 0 & f_{68} & f_{69} \\ f_{71} & f_{72} & 0 & f_{74} & 0 & 0 & f_{77} & f_{78} & f_{79} \\ f_{81} & f_{82} & 0 & f_{84} & 0 & 0 & 0 & f_{88} & f_{89} \\ f_{91} & f_{92} & 0 & f_{94} & f_{95} & 0 & 0 & f_{98} & f_{99} \end{pmatrix} \tag{52}$$

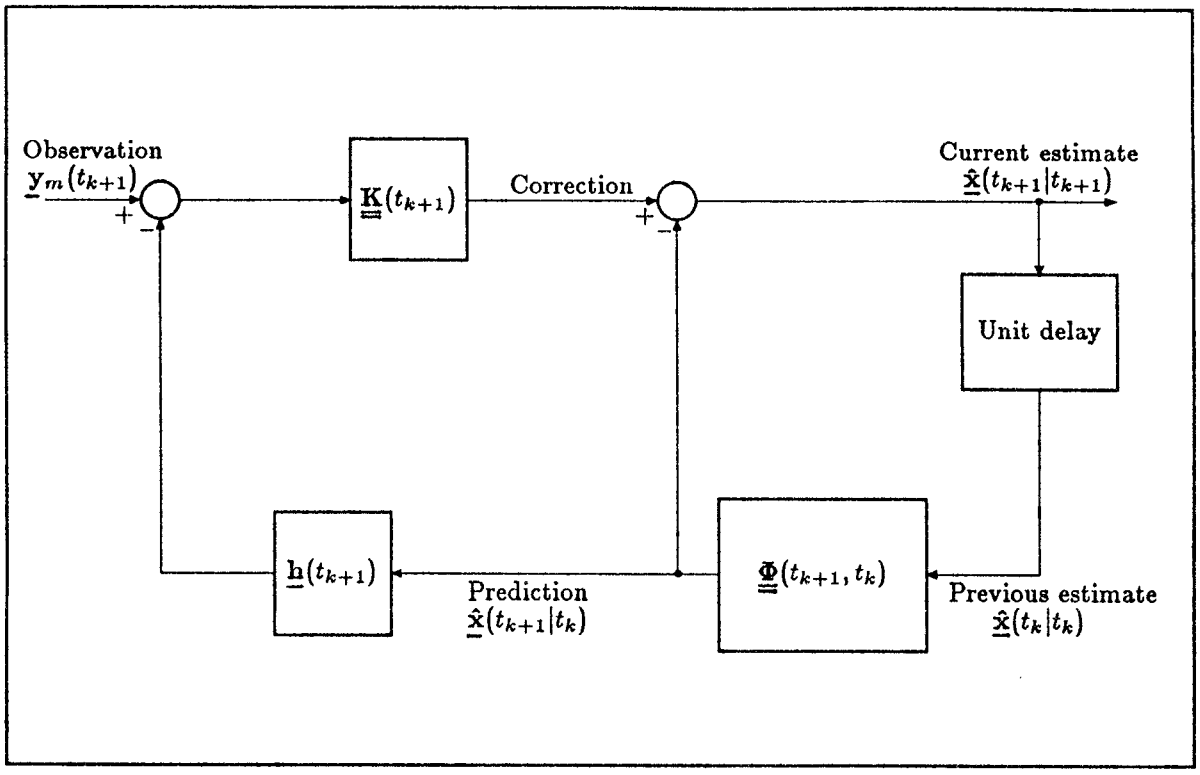

Figure 2. Block diagram of the discrete extended Kalman filter algorithm.

When only on-line measurements are made, the Jacobian of the measurements equations $\underline{\underline{J}}_h$ is

$$\underline{\underline{J}}_h = \begin{pmatrix} h_{11} & h_{12} & 0 & h_{14} & 0 & 0 & 0 & h_{18} & h_{19} \\ 0 & 0 & 0 & 0 & 0 & 0 & 0 & 0 & 1 \end{pmatrix} \tag{53}$$

Note that the methanol measurement (y_{ml}) is a function of five state variables. In the case where off-line measurements are also included, the measurement Jacobian takes on a very simple form

$$\underline{\underline{J}}_h = \begin{pmatrix} h_{11} & h_{12} & 0 & h_{14} & 0 & 0 & 0 & h_{18} & h_{19} \\ 0 & 0 & 0 & 0 & 0 & 0 & 0 & 0 & 1 \\ 0 & -1 & 0 & 0 & 0 & 0 & 0 & 0 & 0 \\ 0 & 0 & 1 & 0 & 0 & 0 & 0 & 0 & 0 \\ 0 & 0 & 0 & 0 & 0 & 1 & 1 & 0 & 0 \\ 0 & 0 & 0 & 1 & 2 & 1 & 0 & 0 & 0 \\ -2 & 0 & 0 & 2 & 2 & 1 & 1 & 0 & 0 \end{pmatrix} \tag{54}$$

The f_{ij} and h_{ij} for $\underline{\underline{J}}_f$ and $\underline{\underline{J}}_h$ are given in Khan (1986).

Observability

In any state estimation scheme, the question of observability must be answered first. According to Ray (1981), a system is completely observable if it is possible to determine all the state variables at some time t_o based on a knowledge of the system output $\underline{y}_m(t)$ and control $\underline{u}(t)$ over some finite interval. It is impossible to design a state estimation algorithm for a system which is not observable. It can be shown that a discrete system is completely observable on $[t_o, t_f]$ if the symmetric Gramian matrix, defined by

$$\underline{\underline{M}}(k_o, k_f) = \sum_{k=k_o}^{k_f} \underline{\underline{\Phi}}^T(k, k_o)\underline{\underline{M}}^T(k)\underline{\underline{M}}(k)\underline{\underline{\Phi}}(k, k_o) \tag{55}$$

is positive definte or nonsingular. For constant-coefficient systems, it can be shown [Kalman (1960)] that a discrete constant system is completely observable if and only if the rank of the observability matrix $\underline{\underline{L}}_o$ is n (n is the number of states),

$$\underline{\underline{L}}_o = [\underline{\underline{M}}^T | \underline{\underline{\Phi}}^T \underline{\underline{M}}^T | (\underline{\underline{\Phi}}^T)^2 \underline{\underline{M}}^T | \ldots | (\underline{\underline{\Phi}}^T)^{n-1} \underline{\underline{M}}^T] \tag{56}$$

where $\underline{\underline{M}}$ and $\underline{\underline{\Phi}}$ have already been defined in eq. (51). For a continuous stirred tank reactor (CSTR), $\underline{\underline{\Phi}}$ and $\underline{\underline{M}}$ are both constant at steady state; thus it is possible to use the observability matrix as it is defined above. In the present case, n = 9, and the rank of $\underline{\underline{L}}_o$ for the transesterification reactor model as proposed is indeed 9; the determination of the rank of $\underline{\underline{L}}_o$ is given in more detail in Khan (1986).

Process Parameters

In order to simulate the transesterification reactor model here as closely as possible to industrial reactors, the parameters listed in Table 3 have been chosen to reflect actual operating and physical conditions. The main operating variables would include the inlet EG/DMT ratio, residence time (or inlet flow rate), inlet catalyst concentration, and heating medium temperature. With respect to these four variables, the base case chosen is

Reactor Volume: 1.0 L

EG/DMT Mole Raio: 1.6

Residence Time: 3 hr

Inlet Catalyst Concentration: 1.08×10^{-3} mol/L

Heating Medium Temperature: $180^{\circ}C$

Variations thereof shall be introduced to ascertain the effect of each variable on the reactor states. For the purpose of simulating measurement noise, the standard deviation of the measurement devices are required. For a type J thermocouple (iron-constantan) a $1.2^{\circ}C$ deviation in the temperature range of interest here ($160\text{-}240^{\circ}C$) is typical [Omega Handbook, 1984]. The standard deviation of the condensate measurement was taken to be approximately 10mL/hr. For the off-line measurements, the measured concentrations were assumed to fall within five percent of the actual concentrations. In dimensionless form, the standard deviations for all the measurements (two on-line measurements and five off-line measurements) become

$$\begin{aligned} \sigma_1 &= 0.03 \\ \sigma_2 &= 0.09 \\ \sigma_3 &= 0.02 \\ \sigma_4 &= 0.0004 \\ \sigma_5 &= 0.0004 \\ \sigma_6 &= 0.043 \\ \sigma_7 &= 0.06 \end{aligned} \tag{57}$$

The dynamic modeling equations were solved deterministically using the fourth order Runge-Kutta method to generate the true process state trajectory. The initial conditions for all the state variables came from the appropriate steady state profiles. On-line measurements used to operate the filter were made at a rate of once every 0.005 dimensionless time increments (about 1 minute in real time for the base case; more frequently for cases involving shorter residence times). The initial conditions of the estimator were deliberately chosen as poor initial state estimates of the actual system states. When off-line measurements were incorporated, it was assumed that analysis results were returned 24 hours after the sampling. When the results of the off-line analysis were made available, the filtering estimates were recomputed starting at the time the sample was actually taken. In order to model white noise in the measurements, a pseudo-random number generator was used to corrupt the actual measured value (obtained from the solution to the dynamic state equations) with a small perturbation. The perturbation was assumed to fall within three standard deviations of the actual measurement. Therefore, the noise-corrupted trajectory then modeled the real process. As a final precaution the error covariance matrix was made symmetric at every time step according to the recommendation of Nahi (1976):

$$\underline{\underline{P}} = 1/2 \ (\underline{\underline{P}}^T + \underline{\underline{P}}) \qquad (58)$$

Note that $\underline{\underline{P}}(t_k | t_k)$ should always be symmetric but computer round-off error prevents it from being exactly so all the time.

In addition to the measurement covariance matrix $\underline{\underline{Q}}$ and the initial values of the state estimates, $\underline{x}(t_o|t_o)$, the extended Kalman filter requires certain tuning parameters in the form of the initial error covariance matrix $\underline{\underline{P}}_o$ and the covariance matrix of the process noise $\underline{\underline{R}}$. The measurement covariance matrix simply contains the variances of the measuring instruments along the diagonal. For the case of semicontinuous on-line measurements, it takes on the form

$$\underline{\underline{Q}} = \begin{pmatrix} 0.0009 & 0 \\ 0 & 0.0081 \end{pmatrix} \tag{59}$$

When additional off-line measurements are also made the measurement covariance matrix takes the following form:

$$\underline{\underline{Q}} = \begin{pmatrix} 0.0009 & 0 & 0 & 0 & 0 & 0 & 0 \\ 0 & 0.0081 & 0 & 0 & 0 & 0 & 0 \\ 0 & 0 & 0.0004 & 0 & 0 & 0 & 0 \\ 0 & 0 & 0 & 1.6\times10^{-7} & 0 & 0 & 0 \\ 0 & 0 & 0 & 0 & 1.6\times10^{-7} & 0 & 0 \\ 0 & 0 & 0 & 0 & 0 & 0.0018 & 0 \\ 0 & 0 & 0 & 0 & 0 & 0 & 0.0324 \end{pmatrix} \tag{60}$$

The values for $\underline{\underline{P}}_o$ and $\underline{\underline{R}}$ were found more or less by trial and error; choices for these two matricies had a substantial impact on the results generated. The form of these matricies is as follows,

$$\underline{\underline{\mathbf{P}}}_{o} = \begin{pmatrix} P_{11} & 0 & 0 & 0 & 0 & 0 & 0 & 0 & 0 \\ 0 & P_{22} & 0 & 0 & 0 & 0 & 0 & 0 & 0 \\ 0 & 0 & P_{33} & 0 & 0 & 0 & 0 & 0 & 0 \\ 0 & 0 & 0 & P_{44} & 0 & 0 & 0 & 0 & 0 \\ 0 & 0 & 0 & 0 & P_{55} & 0 & 0 & 0 & 0 \\ 0 & 0 & 0 & 0 & 0 & P_{66} & 0 & 0 & 0 \\ 0 & 0 & 0 & 0 & 0 & 0 & P_{77} & 0 & 0 \\ 0 & 0 & 0 & 0 & 0 & 0 & 0 & P_{88} & 0 \\ 0 & 0 & 0 & 0 & 0 & 0 & 0 & 0 & P_{99} \end{pmatrix} \tag{61}$$

$$\underline{\underline{\mathbf{R}}} = \begin{pmatrix} R_{11} & 0 & 0 & 0 & 0 & 0 & 0 & 0 & 0 \\ 0 & R_{22} & 0 & 0 & 0 & 0 & 0 & 0 & 0 \\ 0 & 0 & R_{33} & 0 & 0 & 0 & 0 & 0 & 0 \\ 0 & 0 & 0 & R_{44} & 0 & 0 & 0 & 0 & 0 \\ 0 & 0 & 0 & 0 & R_{55} & 0 & 0 & 0 & 0 \\ 0 & 0 & 0 & 0 & 0 & R_{66} & 0 & 0 & 0 \\ 0 & 0 & 0 & 0 & 0 & 0 & R_{77} & 0 & 0 \\ 0 & 0 & 0 & 0 & 0 & 0 & 0 & R_{88} & 0 \\ 0 & 0 & 0 & 0 & 0 & 0 & 0 & 0 & R_{99} \end{pmatrix} \tag{62}$$

These choices and the subsequent results are more completely detailed in the next section. Note that $\underline{\underline{R}}$ and $\underline{\underline{Q}}$ may both be variable with time and cause no difficulty [Wells (1971)], but in this study, they were assumed constant as given.

RESULTS

The simulation of the melt transesterification reactor model incorporating the extended Kalman filter was carried out for the following cases in which step changes in the operating conditions were introduced:

Case 1: With two on-line measurements only.

$P_{ii} = 10^{-8}$ for i = 1, 2, ..., 9

$R_{ii} = 10^{-4}$ for i = 1, 2, ..., 9

Case 2: Same as Case 1 but with 5 additional off-line measurements (delay time = 24 hrs).

The filter starting point in all cases was

DMT Conversion: 0.5

EG Conversion: 0.5

[DEG] = 0.0 mol/L, [MHET] = 0.5 mol/L,

[BHET] = 0.5 mol/L, [HTPA] = 0.0 mol/L,

[MTPA] = 0.0 mol/L, $[C_{cat}] = 1.08 \times 10^{-3}$ mol/L

Reactor temperature = 180°C

Case A1. Figure 3 shows the transient response along with the nonlinear state estimate of the transesterification reactor to a step change in heating medium temperature in the absence of any off-line concentration measurements. The reactor is operated at steady state prior to the step change. Here the solid lines represent the true states and the dotted lines the filter response. Of the nine state variables, DMT conversion, EG conversion, DEG concentration, and MHET concentration are the most important and their transients are shown in Figure 3. The concentration of MHET (half-esterfied DMT) in the

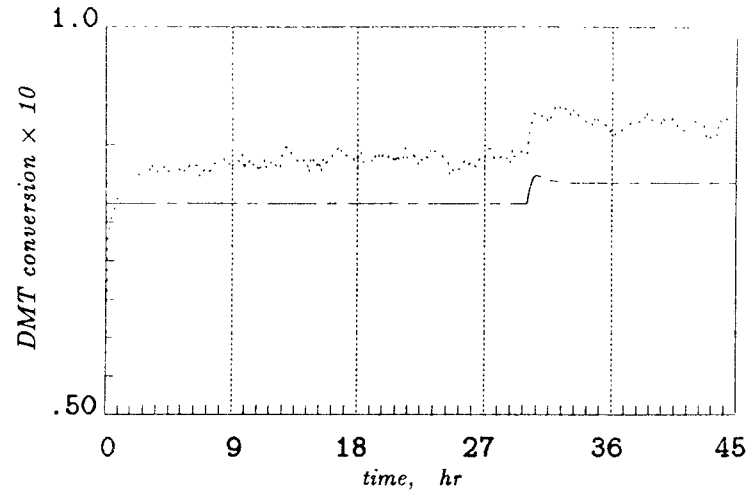

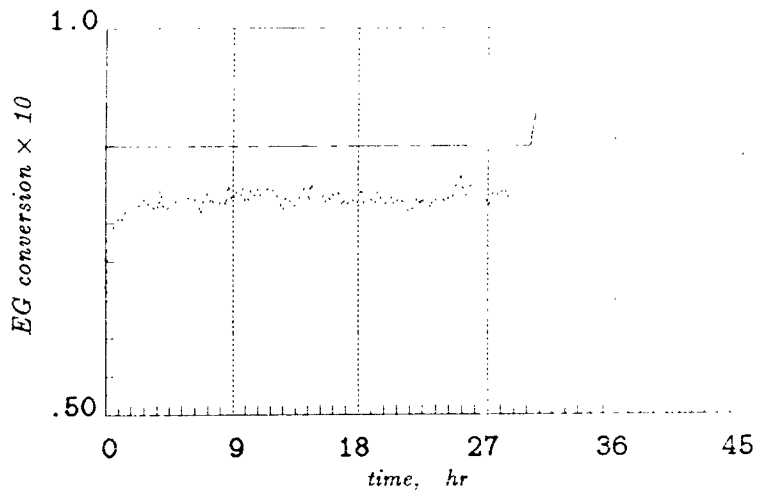

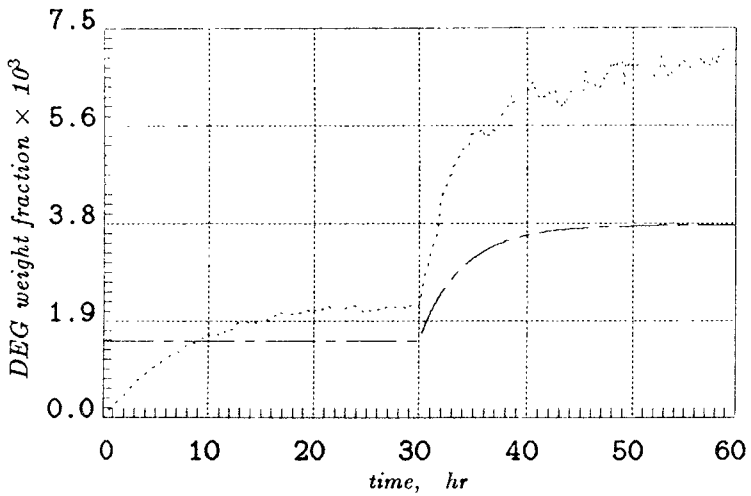

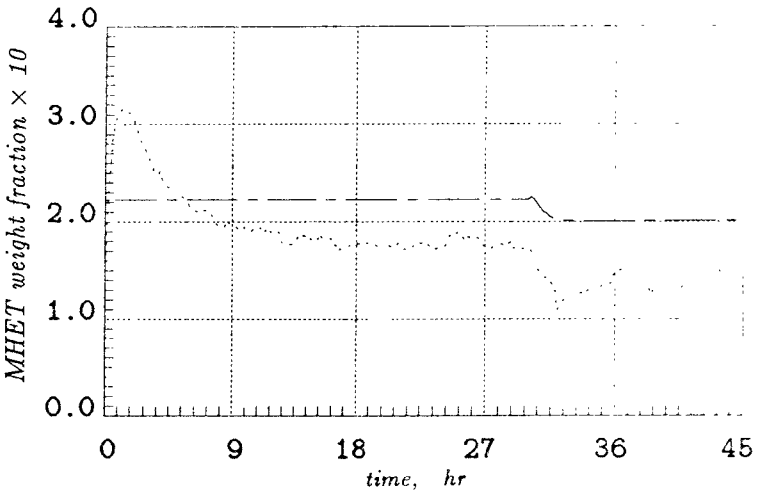

Figure 3: *(Case 1) Filter response to step change in heating medium temperture from 180°C to 200°C with only two on-line measurements.*

transesterification product has an enormous impact on the molecular weight of polyesters to be produced in the second stage (Ault and Mellichamp, 1972). The initial covariances (P_{ii} and R_{ii}) used in this simulation correspond to the case with large modeling error. Note that the prediction of property parameters as shown in Figure 3 is not quite satisfactory. This is because those state variables are only detectable when two on-line measurements (temperature and methanol flow rate) are all that is available.

Case 2. When the two on-line measurements (temperature and methanol flow rate) are complemented by five additional off-line measurements, the filter performance is significantly improved. Figure 4 shows the filter response to the same step disturbance as in Figure 3. Although 24 hours of measurement delay (indicated by the solid black dots) exists, the estimation of the reactor states is excellent [Such a measurement delay (i.e. 24 hrs) is quite realistic from a practical point of view (Yamada et al., 1986)].

Similar simulations were conducted for a step disturbance in the feed EG/DMT mole ratio from 1.6 to 2.0. Figures 5 and 6 show the reactor transients without and with five additional off-line measurements, respectively. Again, excellent filter performance is observed with five additional delayed off-line measurements. It is also interesting to note that increasing the EG/DMT ratio resulted in a significant increase in DEG concentration.

The extended Kalman filter is further capable of accomodating pulse disturbances in reactor operating conditions.

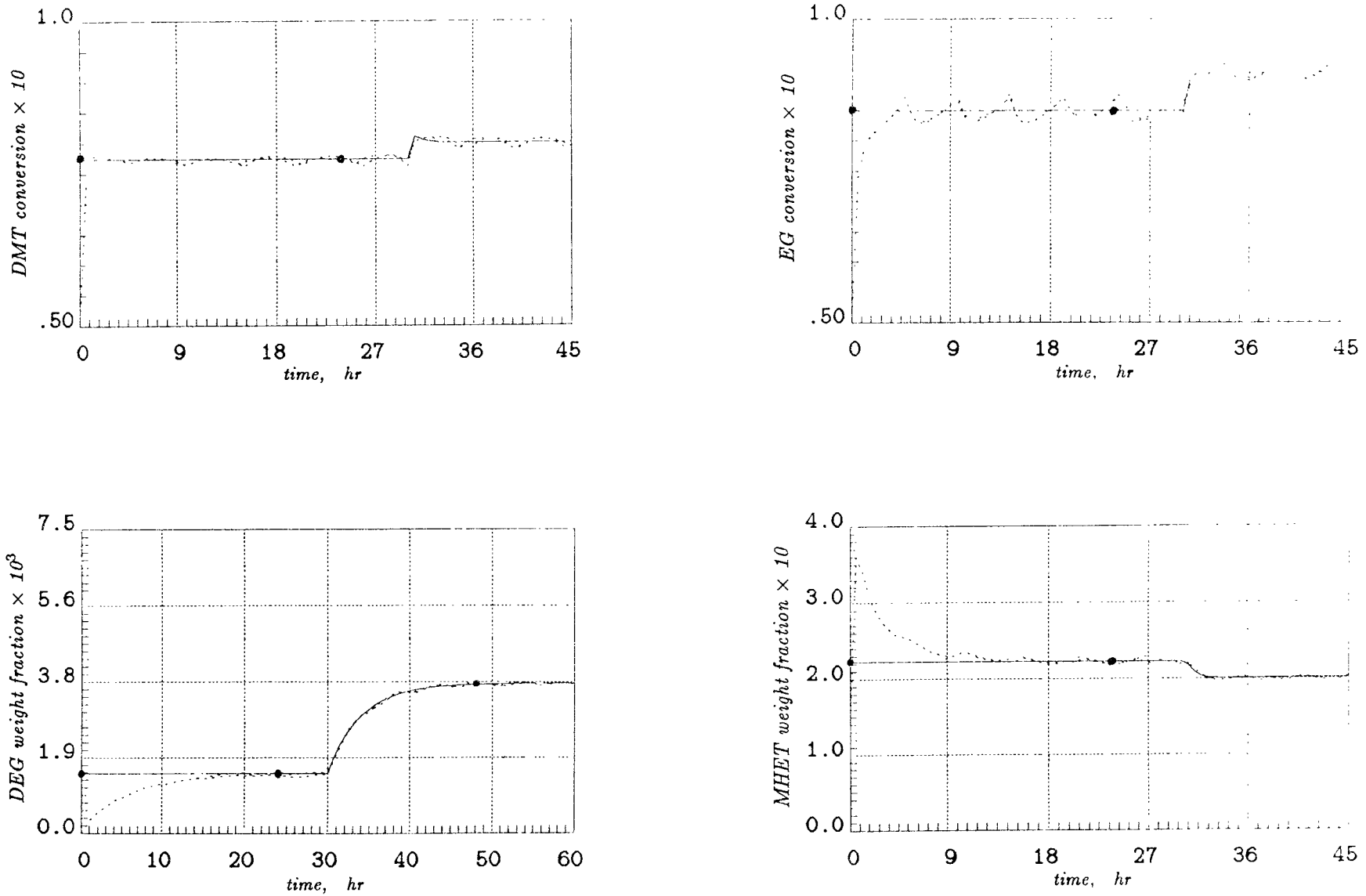

Figure 4: *(Case 2) Filter response to step change in heating medium temperture from 180°C to 200°C with two on-line measurements and five off-line measurements.*

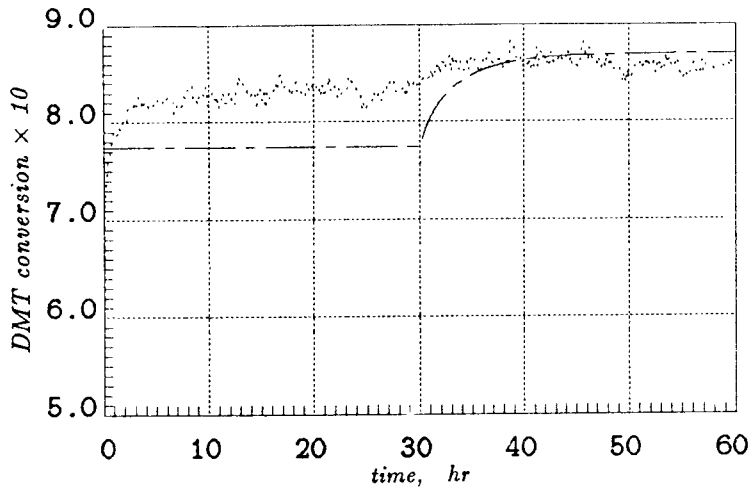

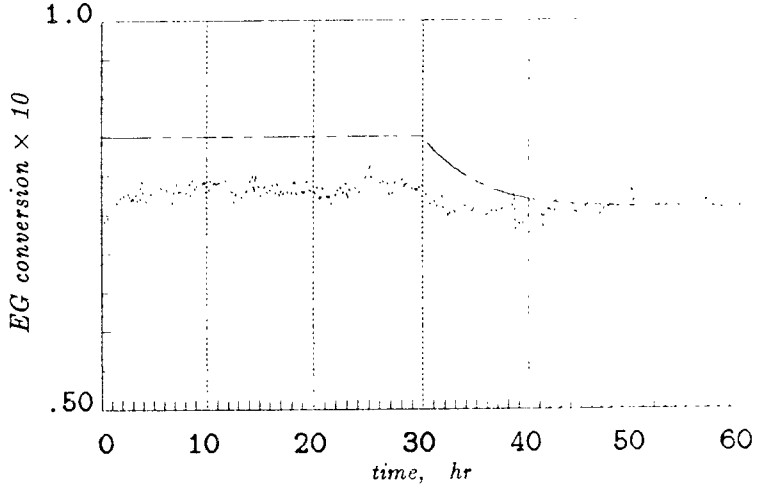

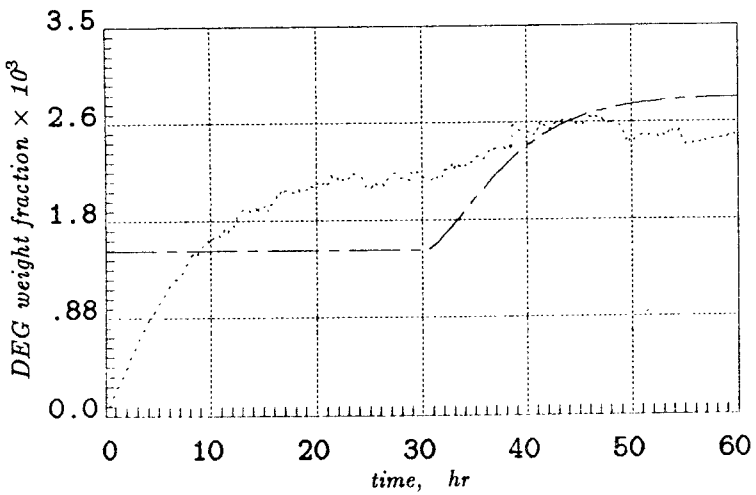

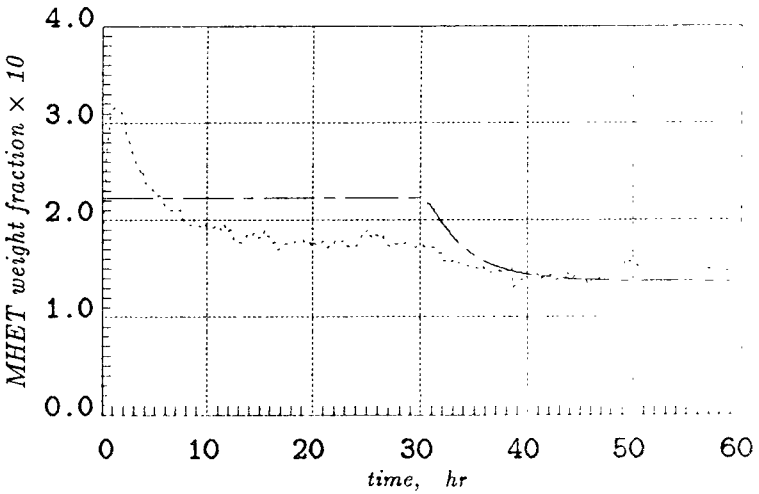

Figure 5: *(Case 1) Filter response to step change in feed EG/DMT mole ratio from 1.6 to 2.0 with only two on-line measurements.*

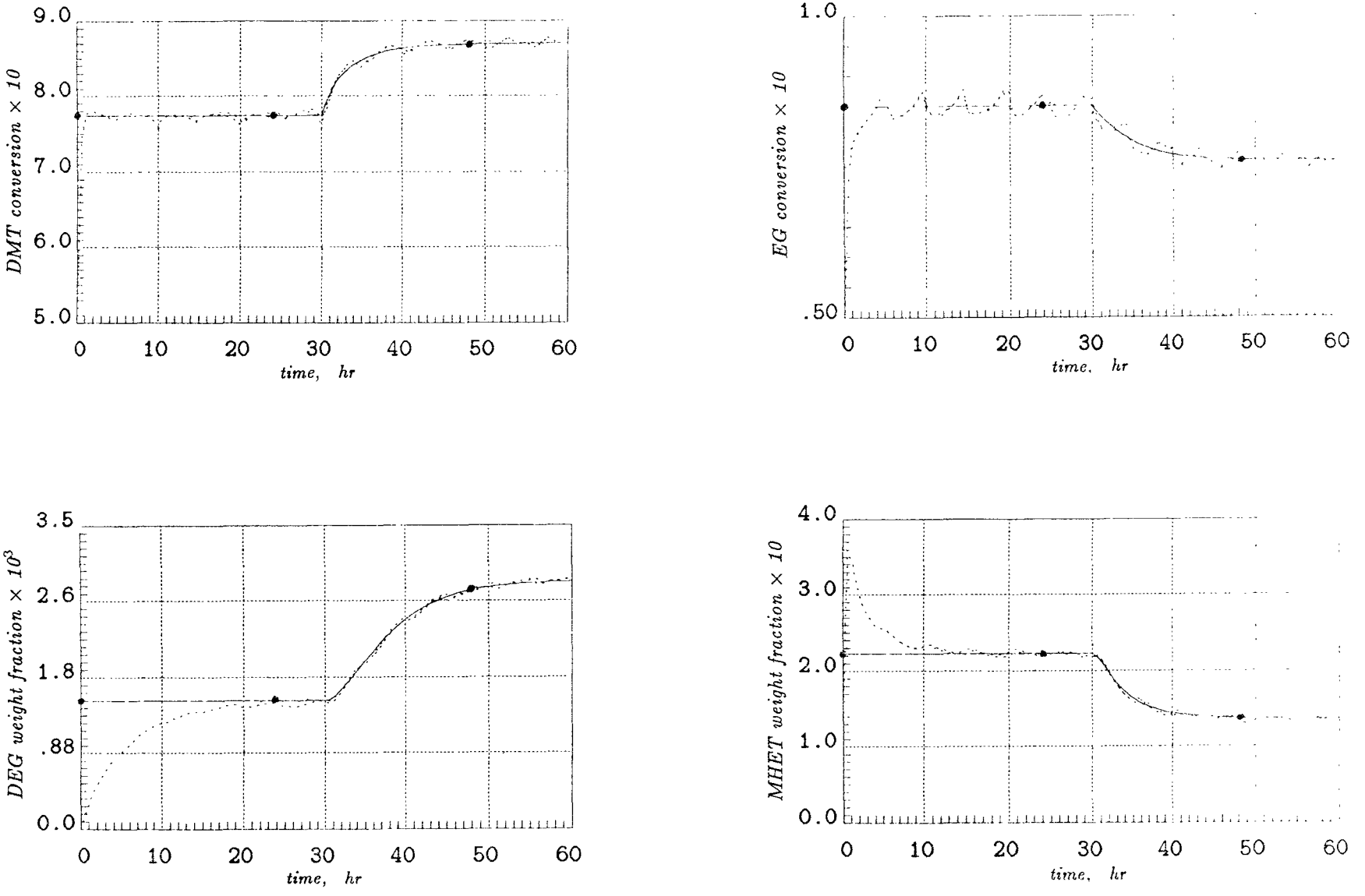

Figure 6: *(Case 2) Filter response to step change in feed EG/DMT mole ratio from 1.6 to 2.0 with two on-line measurements and five off-line measurements.*

Figures 7 and 8 illustrate the filter response to a six hour pulse in the feed EG/DMT molar ratio with only two on-line measurements and with five additional off-line measurements, respectively. Note that once the state estimator converges to the true solution, variations in the state variables can be predicted satisfactorily for such relatively short pulse disturbance. Table 3 lists the numerical values of physical constants and parameters used in the simulations.

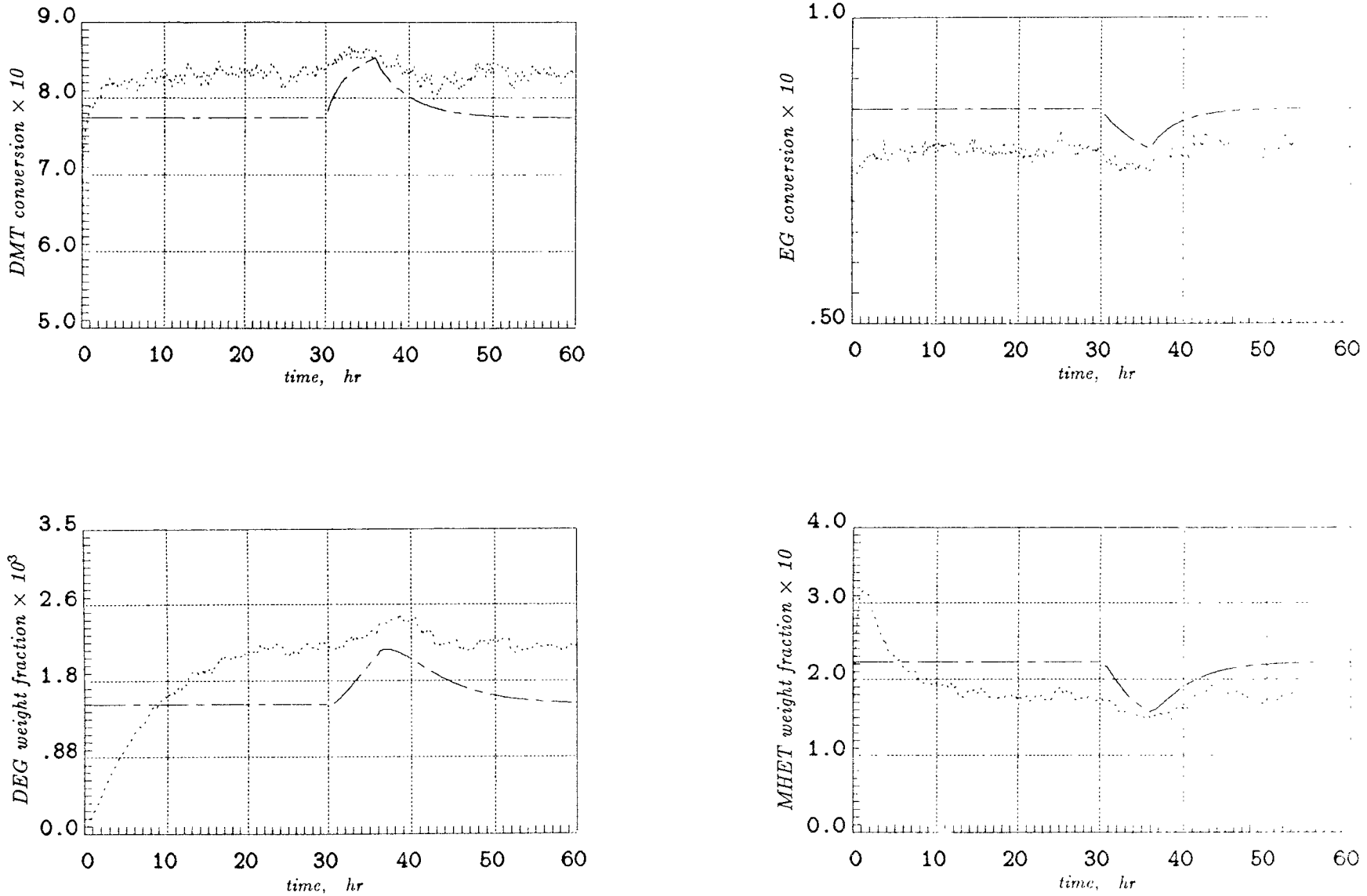

Figure 7: *Filter response to a six hour pulse in feed EG/DMT mole ratio with only two on-line measurements.*

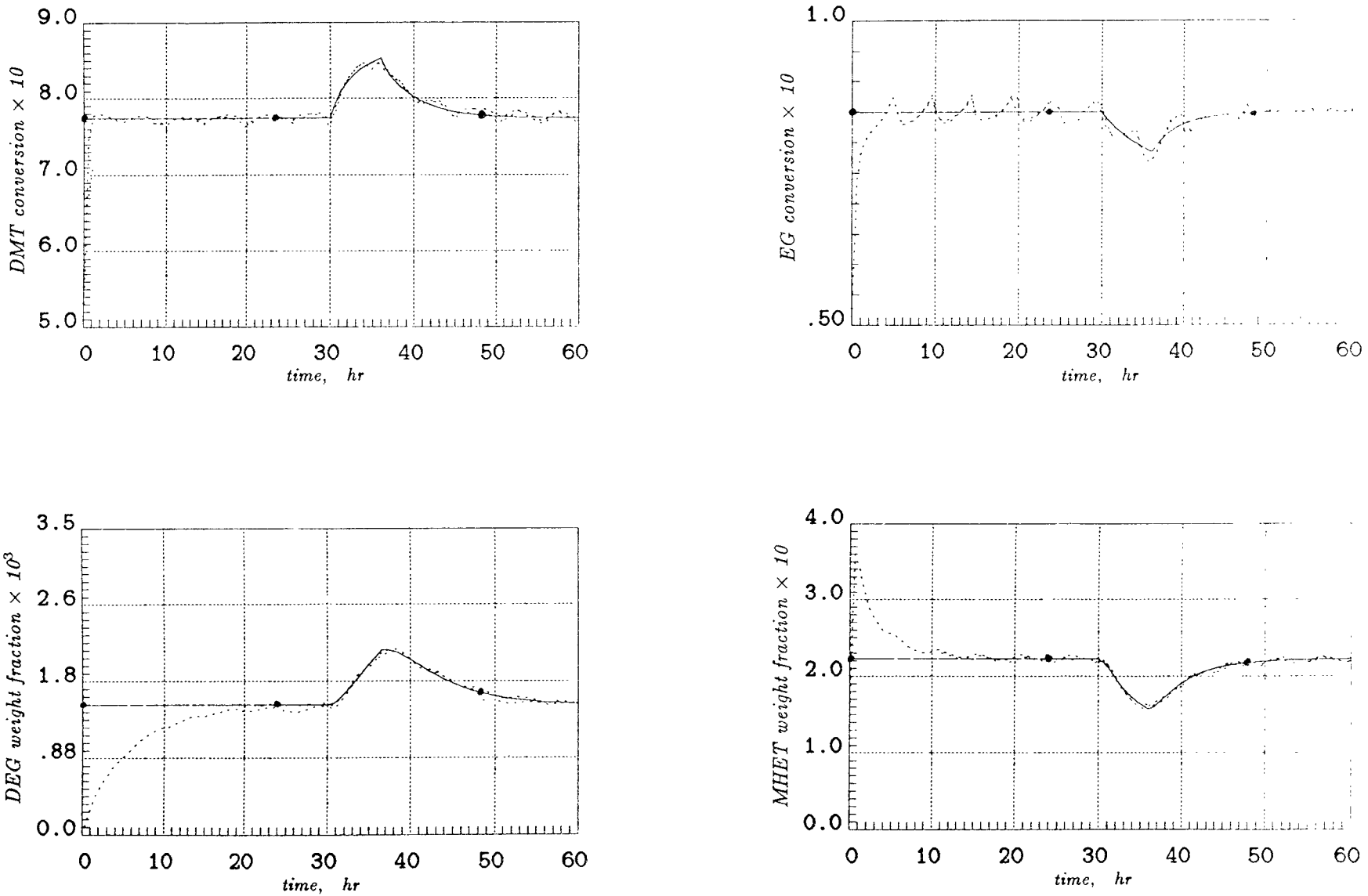

Figure 8: *Filter response to a six hour pulse in feed EG/DMT mole ratio with two on-line measurements and five off-line measurements.*

Table 3: *Numerical values of physical constants and parameters.*

A_1	8.8513×10^9	$\frac{L^2}{mol^2 hr}$	[1]*
A_2	6.0531×10^9	$\frac{L^2}{mol^2 hr}$	[1]
A_3	1.3020×10^{11}	$\frac{L^2}{mol^2 hr}$	[2]
A_c	574.0	cm^2	
C_p	0.245	$\frac{cal}{g^\circ K}$	[3]
$C_{p_{Mg}}$	12.60	$\frac{cal}{mol^\circ K}$	[3]
E_1	14340.0	$\frac{cal}{mol}$	[1]
E_2	14784.0	$\frac{cal}{mol}$	[1]
E_3	29800.0	$\frac{cal}{mol}$	[2]
ΔH_1	1400.0	$\frac{cal}{mol}$	[4]
ΔH_2	1400.0	$\frac{cal}{mol}$	[4]
ΔH_3	0.0	$\frac{cal}{mol}$	[4]
ΔH_4	0.0	$\frac{cal}{mol}$	[4]
ΔH_v	8936.0	$\frac{cal}{mol}$	[3]
T_k	450.0	$^\circ K$	
T_r	298.15	$^\circ K$	
U_o	10.0	$\frac{cal}{cm^2 hr^\circ K}$	[3]
$\hat{V}_M$	0.05363	$\frac{L}{mol}$	[3]
ρ	1.11	$\frac{g}{cm^3}$	
ρ_1	1.11	$\frac{g}{cm^3}$	
ρ_D	1.088	$\frac{g}{cm^3}$	[5]

* *[1] Datye and Raje (1985). [2] Ravindranath and Mashelkar (1982; a,b). [3] Perry and Green (1984). [4] Challa (1960).and [5] Du Pont Co. (1985)*

CONCLUDING REMARKS

A nonisothermal dynamic model for the melt transesterification of DMT with EG has been developed. The model accounts for the variable reactor effluent flow due to the continuous removal of transesterification condensate (methanol) and further incorporates the formation of diethylene glycol which is the major unwanted reaction side product. The extended Kalman filter was used to reconstruct the state variables with a limited number of on-line measurements and delayed laboratory off-line analysis. Although relatively large modeling errors were introduced in the simulation runs, the performance of the filter was greatly improved when on-line measurements were supplemented with infrequent off-line analysis. This indicates that the control of side product formation may be effectively achieved by integrating a state estimation algorithm with an appropriate reactor control strategy.

Acknowledgement

This work was supported by the National Science Foundation (Grant CBT-8504874) and in part by the Computer Science Center at the University of Maryland and the Systems Research Center of the University of Maryland.

Literature Cited

Ault, J. W., and D. A. Mellichamp, "Complex Linear Polycondensation. I. Semi-batch Reactor", Chem. Eng. Sci., 27, 2219 (1972).

Challa, G., "Ester Interchange Equilibria From Dimethyl Terephthalate And Ethylene Glycol", Rec. Trav. Chim., 79, 90 (1986).

Datye, K. V., and H. M. Raje, "Kinetics of Transesterification of Dimethylene Terephthalate with Ethylene Glycol", J. Appl. Poly. Sci., 30, 205 (1985).

Dupont Co., "DMT Material Safety and Data Sheet", Polymer Intermediates Dept., #E-77976 (1985).

Gavalas, G. R., and J. H. Seinfeld, "Sequential EStimation of States and Kinetic Parameters in Tubular Reactors with Catalyst Decay", Chem. Eng. Sci., 24, 625 (1969).

Jazwinski, A. H., "Stochastic Processes and Filtering Theory", Academic Press, New York (1970).

Kalman, R. E., "A New Approach to Linear Filter and Prediction Problems", ASME Transactions, Series D: J. Basic Eng., 82, 35 (1960).

Khan, A. A., "Modeling and State Estimation of the Transesterification Stage in a Continuous Polycondensation Process for Polyethylene Terephthalate", M.S. Thesis, University of Maryland, College Park (1986).

Nahi, N. E., "Estimation Theory and Applications", Robert E. Krieger Publishing Co., Huntington, New York (1976).

Omega Temperature Measurement Handbook and Encyclopedia, Stamford, Connecticut (1984).

Perry, R. H., and D. W. Green, "Perry's Chemical Engineers' Handbook", 6th ed., McGraw-Hill, New York (1984).

Ravindranath, K. and R. A. Mashelkar, "Modeling of Poly(ethylene Terephthalate) Reactors. I. A Semibatch Ester Interchange Reactor", J. Appl. Poly. Sci., 26, 3179 (1981).

Ravindranath, K., and R. A. Mashelkar, "Modeling of Poly(ethylene Terephthalate) Reactors. II. A Continuous Tranesterification Process", J. Appl. Poly. Sci., 27, 471 (1982, a).

Ravindranath, K., and R. A. Mashelkar, "Modeling of Poly(ethylene Terephthalate) Reactors. III. A Semibatch Prepolymerization Process", J. Appl. Poly. Sci., 27, 2625 (1982, b).

Ray, W. H., "Advanced Process Control", McGraw-Hill, New York (1981).

Sage, A. P., and J. L. Melsa, "Estimation Theory with Applications to Communications and Control", McGraw-Hill, New York (1971).

Schuler, H. and S. Zhang, "Real-Time Estimation of the Chain Length Distribution in a Polymerization Reactor", Chem. Eng. Sci., 40, 1891 (1985).

Wells, C. H., "Application of Modern Estimation and Identification Techniques to Chemical Processes", A.I.Ch.E.J., 17, 966 (1971).

Yamada, T., Y. Imamura and O. Makimura, "A Mathematical Model for Computer Simulation of the Direct Continuo9us Esterification Process Between Terephthalic Acid and Ethylene Glycol. Part II. Reaction Rate Constants", Poly. Eng. Sci., 26, 708 (1986).

Figure Captions

Figure 1 Schematic diagram of continuous melt PET polymerization process.

Figure 2 Block diagram of the discrete extended Kalman filter algorithm.

Figure 3 (Case 1) Filter response to step change in heating medium temperature from 180°C to 200°C with only two on-line measurements (solid line; true state, dotted line; filter estimate).

Figure 4 (Case 2) Filter response to step change in heating medium temperature from 180°C to 200°C with two on-line measurements and five off-line measurements (solid line; true state, dotted line; filter estimate).

Figure 5 (Case 1) Filter response to step change in feed EG/DMT mole ratio from 1.6 to 2.0 with only two on-line measurements (solid line; true state, dotted line; filter estimate).

Figure 6 (Case 2) Filter response to step change in feed EG/DMT mole ration from 1.6 to 2.0 with two on-line measurements and five off-line measurements (solid line; true state, dotted line; filter estimate).

Figure 7 Filter response to a six hour pulse in feed EG/DMT mole ratio from 1.6 to 2.0 with only two on-line measurements (solid line; true state, dotted line; filter estimate).

Figure 8 Filter response to a six hour pulse in feed EG/DMT mole ratio from 1.6 to 2.0 with two on-line measurements and five off-line measurements (solid line; true state, dotted line; filter estimate).

NOTATION

A_1 frequency factor for reaction 1, L^2mol^2/hr

A_2 frequency factor for reaction 2, L^2mol^2/hr

A_3 frequency factor for reactions 3 and 4, L^2mol^2/hr

A_c heat transfer area, cm_2

B_i dimensionless adiabatic temperature rise for reaction i

B_v dimensionless heat of vaporization for methanol

C_{cat} reactor catalyst concentration, mol/L

C_{cato} feed catalyst concentration, mol/L

C_p heat capacity of reaction mixture, $cal/g/^oK$

C_{PMg} molar heat capacity of methanol gas, $cal/gmol/^oK$

D reactor DMT concentration, mol/L

D_o feed DMT concentration, mol/L

Da Damkohler number

E_1 activation energy for reaction 1, cal/gmol

E_2 activation energy for reaction 2, cal/gmol

E_3 activation energy for reactions 3 and 4, cal/gmol

G reactor ethylene glycol concentration, mol/L

G_o feed ethylene glycol concentration, mol/L

G_D reactor diethylene glycol concentration, mol/L

G_{Do} feed diethylene glycol concentration, mol/L

ΔH_1 heat of reaction 1 at T_r, cal/gmol

ΔH_2 heat of reaction 2 at T_r, cla/gmol

ΔH_3 heat of reaction 3 at T_r, cal/gmol

ΔH_4 heat of reaction 4 at T_r, cal/gmol

ΔH_v heat of vaporization for methanol at T_r, cal/gmol

k_1 reaction rate constant for reaction 1, L^2mol^2/hr

k_2 reaction rate constant for reaction 2, L^2nik^2/hr

k_3 reaction rate constant for reactions 3 and 4, L^2mol^2/hr

M methanol concentration, mol/L

P_1 reactor BHET concentration, mol/L

P_{1o} feed BHET concentration, mol/L

Q_1 reactor HTPA concentration, mol/L

Q_{10} feed HTPA concentration, mol/L

q dimensionless liquid exit flow

q_o feed flow rate, L/hr

q_1 exit liquid flow rate, L/hr

R gas constant, cal/gmol/^oK

R_1 reactor MHET concentration, mol/L

R_{10} feed MHET concentration, mol/L

r_1 ratio of reaction rate constants k_1 and k_3 at T_k

r_2 ratio of reaction rate constnats k_2 and k_3 at T_k

T reactor temperature, ^oK

T_o feed temperature, ^oK

T_1 reactor MTPA concentration, mol/L

T_{10} feed MTPA concentration, mol/L

T_h heating medium temperature, ^oK

T_k non-dimensionalizing base temperature, ^oK

T_r reference temperature, ^oK

t' time, hr

t dimensionless time

U_o overall heat transfer coefficient, cal/cm^2/^oK/hr

V reactor working volume, L

$\hat{V}_M$ molar volume of methanol in desired temperature range, L/mol

W_D molecular weight of DMT, g/gmol

W_G molecular weight of EG, g/gmol

W_M molecular weight of methanol, g/gmol

x_1 DMT conversion

x_2 EG conversion

x_3 dimensionless DEG concentration

x_4 dimensionless MHET concentration

x_5 dimensionless BHET concentration

x_6 dimensionless HTPA concentration

x_7 dimensionless MTPA concentration

x_8 catalyst conversion

x_9 dimensionless reactor temperature

y_1 dimensionless feed temperature

y_2 dimensionless heating medium temperature

y_3 dimensionless methanol molar volume

y_4 ratio of inlet to reactor densities

y_5 ratio of outlet to reactor densities

y_6 dimensionless methanol heat capacity

y_7 dimensionless reference temperature

z_2 feed EG/DMT ratio

z_3 dimensionless feed DEG concentration

z_4 dimensionless feed MHET concentration

z_5 dimensionless feed BHET concentration

z_6 dimensionless feed HTPA concentration

z_7 dimensionless feed MTPA concentration

Greek Letters

β	dimensionless heat transfer capability
γ	feed catalyst/DMT mole ratio
ρ	reaction mass density, g/L
ρ_o	feed density, g/L
ρ_1	exit flow density, g/L
Γ	dimensionless activation energy
Γ_1	ratio of activation energies E_1 and E_3
Γ_2	ratio of activation energies E_2 and E_3
σ_i	standard deviation of measurement i
θ	residence time, hr

Matricies and Vectors

$\underline{f}$	n-dimensional state vector-valued function
$\underline{h}$	m-dimensional observation vector
$\underline{v}$	m-dimensional observation-noise vector
$\underline{w}$	n-dimensional plant-noise vector
$\underline{x}$	state vector
$\underline{x}_o$	initial value of state vector
$\underline{x}$	vector of state estimates
$\underline{x}_o$	initial value vector for state estimates
$\underline{Y}_m$	m-dimensional observation vector
$\underline{\underline{I}}$	identity matrix
$\underline{\underline{J}}_f$	Jacobian matrix of state equations
$\underline{\underline{J}}_h$	Jacobian matrix of measurement equations
$\underline{\underline{K}}$	Kalman gain
$\underline{\underline{L}}_o$	observability matrix
$\underline{\underline{M}}$	Jacobian matrix of measurement equations symmetric Gramian matrix

$\underline{\underline{P}}$ error covariance matrix

$\underline{\underline{P}}_O$ covariance of initial state errors

$\underline{\underline{Q}}$ covariance of measurement noise

$\underline{\underline{R}}$ covariance of plant noise

$\underline{\underline{\Phi}}$ state transition matrix